Energy & Environmental Science

ANALYSIS

View Article Online
View Journal | View Issue

Cite this: *Energy Environ. Sci.*, 2015, **8**, 1938

Hydrogen or batteries for grid storage? A net energy analysis†

Matthew A. Pellow,*[a] Christopher J. M. Emmott,[bc] Charles J. Barnhart[d] and Sally M. Benson[aef]

Energy storage is a promising approach to address the challenge of intermittent generation from renewables on the electric grid. In this work, we evaluate energy storage with a regenerative hydrogen fuel cell (RHFC) using net energy analysis. We examine the most widely installed RHFC configuration, containing an alkaline water electrolyzer and a PEM fuel cell. To compare RHFC's to other storage technologies, we use two energy return ratios: the electrical energy stored on invested ($ESOI_e$) ratio (the ratio of electrical energy returned by the device over its lifetime to the electrical-equivalent energy required to build the device) and the overall energy efficiency (the ratio of electrical energy returned by the device over its lifetime to total lifetime electrical-equivalent energy input into the system). In our reference scenario, the RHFC system has an $ESOI_e$ ratio of 59, more favorable than the best battery technology available today (Li-ion, $ESOI_e$ = 35). (In the reference scenario RHFC, the alkaline electrolyzer is 70% efficient and has a stack lifetime of 100 000 h; the PEM fuel cell is 47% efficient and has a stack lifetime of 10 000 h; and the round-trip efficiency is 30%.) The $ESOI_e$ ratio of storage in hydrogen exceeds that of batteries because of the low energy cost of the materials required to store compressed hydrogen, and the high energy cost of the materials required to store electric charge in a battery. However, the low round-trip efficiency of a RHFC energy storage system results in very high energy costs during operation, and a much lower overall energy efficiency than lithium ion batteries (0.30 for RHFC, *vs.* 0.83 for lithium ion batteries). RHFC's represent an attractive investment of manufacturing energy to provide storage. On the other hand, their round-trip efficiency must improve dramatically before they can offer the same overall energy efficiency as batteries, which have round-trip efficiencies of 75–90%. One application of energy storage that illustrates the tradeoff between these different aspects of energy performance is capturing overgeneration (spilled power) for later use during times of peak output from renewables. We quantify the relative energetic benefit of adding different types of energy storage to a renewable generating facility using $[EROI]_{grid}$. Even with 30% round-trip efficiency, RHFC storage achieves the same $[EROI]_{grid}$ as batteries when storing overgeneration from wind turbines, because its high $ESOI_e$ ratio and the high EROI of wind generation offset the low round-trip efficiency.

Received 22nd December 2014,
Accepted 8th April 2015

DOI: 10.1039/c4ee04041d

www.rsc.org/ees

Broader context

The rapid increase in electricity generation from wind and solar is a promising step toward decarbonizing the electricity sector. Because wind and solar generation are highly intermittent, energy storage will likely be key to their continued expansion. A wide variety of technology options are available for electric energy storage. One is a regenerative hydrogen fuel cell (RHFC) system that converts electricity to hydrogen by water electrolysis, stores the hydrogen, and later provides it to a fuel cell to generate electric power. RHFC systems are already operating in several dozen locations. In this net energy analysis, we compare the quantity of energy dispatched from the system over its lifetime to the energy required to build the device. We find that, for the same quantity of manufacturing energy input, hydrogen storage provides more energy dispatched from storage than does a typical lithium ion battery over the lifetime of the facility. On the other hand, energy storage in hydrogen has a much lower round-trip efficiency than batteries, resulting in significant energy losses during operation. Even at its present-day round-trip efficiency of 30%, however, it can provide the same overall energy benefit as batteries when storing overgeneration from wind farms.

[a] *Global Climate and Energy Project, Stanford University, Stanford, CA 94305, USA. E-mail: mpellow@stanford.edu*
[b] *Department of Physics, Imperial College London, London, SW7 2AZ, UK*
[c] *Grantham Institute for Climate Change, Imperial College London, London, SW7 2AZ, UK*
[d] *Institute for Energy Studies, Western Washington University, Bellingham, WA 98225, USA*
[e] *Department of Energy Resources Engineering, Stanford University, Stanford, CA 94305, USA*
[f] *Precourt Institute for Energy, Stanford University, Stanford, CA 94305, USA*

† Electronic supplementary information (ESI) available. See DOI: 10.1039/c4ee04041d

1 Introduction

Annual electricity generation from wind and solar power is growing rapidly,[1,2] and can contribute significantly to reducing our society's carbon emissions.[3] However, these technologies present significant challenges to grid operators, including intermittent output and a mismatch between peak output and peak demand, which can result in grid instability, negative pricing, and wasteful curtailment.[4] Grid-scale energy storage enables further growth of these low-emissions generating sources by levelling peak load, increasing the capacity factors of wind and solar installations, and transforming these intermittent generators into grid-dispatchable resources.[5–7] A variety of grid-scale storage technologies are available, including pumped hydro, compressed air, and various types of battery storage.[8–10]

Another technology available for grid-scale energy storage is a regenerative fuel cell, in which energy is stored as hydrogen gas.[11–13] A regenerative hydrogen fuel cell system consists of a water electrolyzer, compressed hydrogen gas storage tanks, and a fuel cell (Fig. 1). The system uses electricity to generate hydrogen from water in an electrolyzer. The hydrogen is stored in high-pressure tanks, and dispatched to the hydrogen fuel cell to generate electricity when desired.

Regenerative hydrogen fuel cells (RHFC's) have several characteristics that are well-suited to large-scale energy storage. They are not subject to geological requirements, which are important restrictions on pumped hydro and compressed air storage. The energy capacity and power capacity of a regenerative fuel cell can be configured independently. Storing energy in hydrogen provides a dramatically higher energy density than any other energy storage medium.[8,10] Hydrogen is also a flexible energy storage medium which can be used in stationary fuel cells (electricity only or combined heat and power),[12,14] internal combustion engines,[12,15,16] or fuel cell vehicles.[17–20] Hydrogen storage has a very low rate of self-discharge, and has therefore been proposed for seasonal storage.[8,21] The cost of energy storage in a regenerative hydrogen fuel cell is already potentially competitive with batteries in an optimized energy arbitrage system.[22] Several dozen RHFC projects have already implemented hydrogen storage, spanning a wide range of energy and power capacities (Fig. 2).[12] The most common configuration among existing systems contains an alkaline water electrolyzer (AWE) and a polymer electrolyte membrane fuel cell (PEMFC).‡

Although there are important benefits when renewable electricity is stored for later use rather than curtailed, we also incur an energy cost when we build the energy storage systems that make this possible. Net energy analysis provides a consistent methodology with which to compare these energetic costs and benefits. Net energy analysis is a life cycle analysis technique that compares the energy output of a device or process to the energy inputs required to manufacture and operate it.[23] Previous work has analyzed the tradeoff between curtailing excess generation

‡ Ref. 12 specified the technologies types of both the electrolyzer and the fuel cell for 38 RHFC systems. These include 15 AWE–PEMFC systems; 10 PEMWE–PEMFC systems; four AWE–ICE systems; four AWE–CHP systems; two AWE–AFC systems; one PEMWE–ICE system; and one AWE–phosphoric acid fuel cell system.

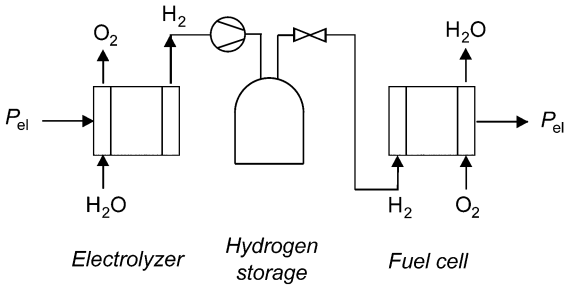

Fig. 1 Schematic of a regenerative hydrogen fuel cell system.

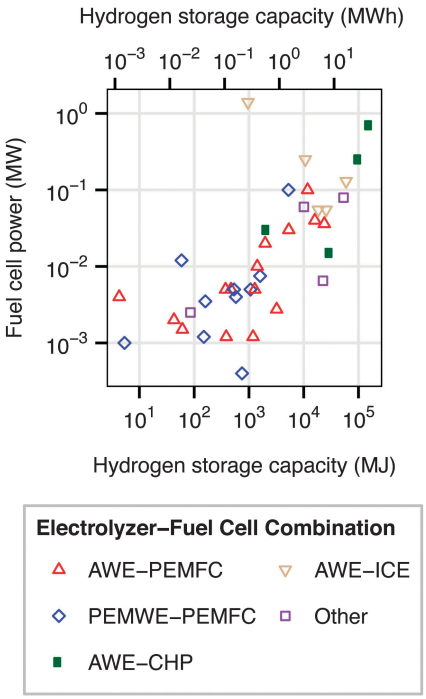

Fig. 2 Power and energy ratings of some existing RHFC systems. "Other" includes systems in which an alkaline water electrolyzer is paired with an alkaline fuel cell or phosphoric acid fuel cell; or a PEM water electrolyzer with an internal combustion engine. Data from ref. 12.

from renewables and building new energy storage to capture it, using the energy stored on invested ($ESOI_e$) ratio of different storage technologies.[24] The $ESOI_e$ ratio is a measure of how much energetic benefit our society receives in exchange for each unit of energy invested in building an energy storage system:

$$ESOI_e = \frac{[\text{Energy dispatched to grid over lifetime}]_{\text{electrical}}}{[\text{Energy required to manufacture}]_{\text{electrical}}} \quad (1)$$

where the subscript "e" denotes quantities of electrical energy. The $ESOI_e$ ratio serves as an apples-to-apples comparison of the net energy balance of different storage technologies, and provides a basis for determining whether building new storage or curtailing overgeneration yields a greater total energy return.

In the present study, we use net energy analysis to compare regenerative hydrogen fuel cells to other storage technologies on the basis of life-cycle energy costs. We first introduce a

model to determine the $ESOI_e$ ratio of a RHFC system as a function of system parameters such as fuel cell efficiency and energy-to-power ratio. We apply this model to a RHFC system containing an alkaline water electrolyzer and a PEM fuel cell, and analyze the impact of different technology and design variables on the system's lifetime energy balance. We then use the model to analyze the energy cost or benefit that results from building new RHFC storage to complement an intermittent renewable generating facility. Finally, we compare it with a lithium ion battery storage system, which has the highest $ESOI_e$ ratio among the battery technologies currently used for grid-scale storage.

2 Methodology

2.1 $ESOI_e$ ratio of a regenerative hydrogen fuel cell

2.1.1 $ESOI_e$ ratio as a function of RHFC operating parameters. The energy stored on invested ($ESOI_e$) ratio of a storage device is the ratio of electrical energy it dispatches to the grid over its lifetime to the embodied electrical energy§ required to build the device.[24]¶ We restate equation (1) as

$$\mathrm{ESOI_e} = \frac{\left[E_{\mathrm{out}}^{\mathrm{life}}\right]_{\mathrm{el}}}{\left[E_{\mathrm{emb}}^{\mathrm{life}}\right]_{\mathrm{el}}} \tag{2}$$

The denominator is the sum of the embodied energies of each individual component of the system. For the regenerative fuel cell system depicted in Fig. 1, the denominator includes terms for the electrolyzer (lyz), hydrogen compressor (comp), hydrogen storage (st), and fuel cell (FC).

$$\mathrm{ESOI_e} = \frac{\left[E_{\mathrm{out}}^{\mathrm{life}}\right]_{\mathrm{el}}}{\left[E_{\mathrm{emb,lyz}}^{\mathrm{life}} + E_{\mathrm{emb,comp}}^{\mathrm{life}} + E_{\mathrm{emb,st}}^{\mathrm{life}} + E_{\mathrm{emb,FC}}^{\mathrm{life}}\right]_{\mathrm{el}}} \tag{3}$$

Each quantity in eqn (3) can be restated in terms of the operating parameters of the system components.

The total lifetime energy output from the regenerative fuel cell is the product of the fuel cell's cumulative operating time, T_{FC}, and its rated power, P_{FC}.‖

$$\left[E_{\mathrm{out}}^{\mathrm{life}}\right]_{\mathrm{el}} = T_{\mathrm{FC}}P_{\mathrm{FC}} \tag{4}$$

In the denominator of eqn (3), each term is the product of a capacity (a quantity of electrolyzer power, storage capacity, or fuel cell power) and an energy intensity (the amount of electrical energy required to manufacture one unit of capacity).

For the electrolyzer embodied energy, we distinguish the contribution from the cell stack (which may need replacement during the system lifetime) from that in the balance of system (BOS; which we assume to be durable throughout the system lifetime). The number of cell stack replacements is given by the ratio of the system lifetime, T_{lyz}, to the operating lifetime of the cell stack, $\tau_{lyz,stack}$. We apply the ceiling function to this ratio (*i.e.* round up to the next integer) to reflect complete (not fractional) stack replacement.

$$E_{\mathrm{emb,lyz}}^{\mathrm{life}} = P_{\mathrm{lyz}}\zeta_{\mathrm{lyz,stack}}\left\lceil\frac{T_{\mathrm{lyz}}}{\tau_{\mathrm{lyz,stack}}}\right\rceil + P_{\mathrm{lyz}}\zeta_{\mathrm{lyz,BOS}} \tag{5}$$

Because the required compressor capacity is determined by the hydrogen flow rate from the electrolyzer, which in turn is determined by the electrolyzer's power capacity, we normalize the energy intensity of the compressor to the power capacity of the electrolyzer. The total embodied energy is the product

$$E_{\mathrm{emb,comp}}^{\mathrm{life}} = P_{\mathrm{lyz}}\zeta_{\mathrm{comp}} \tag{6}$$

The embodied energy of the hydrogen storage tanks is the product of the storage capacity and the energy intensity

$$E_{\mathrm{emb,st}}^{\mathrm{life}} = S\varepsilon_{\mathrm{st}} \tag{7}$$

if we assume that the hydrogen storage tanks last for the full service lifetime of the RHFC system.

For the embodied energy of the fuel cell, we specify the contributions from the cell stack and balance of plant, as with the electrolyzer.

$$E_{\mathrm{emb,FC}}^{\mathrm{life}} = P_{\mathrm{FC}}\zeta_{\mathrm{FC,stack}}\left\lceil\frac{T_{\mathrm{FC}}}{\tau_{\mathrm{FC,stack}}}\right\rceil + P_{\mathrm{FC}}\zeta_{\mathrm{FC,BOS}} \tag{8}$$

Substitution into eqn (3) gives

$$\mathrm{ESOI_e} = \frac{T_{\mathrm{FC}}P_{\mathrm{FC}}}{P_{\mathrm{lyz}}\zeta_{\mathrm{lyz,stack}}\left\lceil\frac{T_{\mathrm{lyz}}}{\tau_{\mathrm{lyz,stack}}}\right\rceil + P_{\mathrm{lyz}}\zeta_{\mathrm{lyz,BOS}} + P_{\mathrm{lyz}}\zeta_{\mathrm{comp}} + S\varepsilon_{\mathrm{st}} + P_{\mathrm{FC}}\zeta_{\mathrm{FC,stack}}\left\lceil\frac{T_{\mathrm{FC}}}{\tau_{\mathrm{FC,stack}}}\right\rceil + P_{\mathrm{FC}}\zeta_{\mathrm{FC,BOS}}} \tag{9}$$

where T_{FC} and T_{lyz} are the cumulative operating durations of the fuel cell and electrolyzer throughout the service life of the storage facility (in s); P_{FC} and P_{lyz} are the electric power ratings of the fuel cell and electrolyzer (in $[MW]_{el}$); S is the storage capacity of the hydrogen tank (in $[MJ]_{LHV}$**); ζ_{lyz}, ζ_{comp} and ζ_{FC} are the electrical energy intensities of electrolyzer, compressor and fuel cell (in $[MJ]_{el}/[MW]_{el}$); ε_{st} is the electrical energy intensity of the hydrogen tank (in $[MJ]_{el}/[MJ]_{LHV}$); and τ_{FC} and τ_{lyz} are the operating lifetimes of the fuel cell stack and electrolyzer stack (in s).

2.1.2 Dependence on energy-to-power ratio. An important characteristic of an energy storage system is the duration of dispatch from the fully charged state. This duration is proportional to the system's energy-to-power ratio. For the RHFC,

§ *I.e.* the quantity of electrical energy that would result if all primary energy inputs were converted to electrical energy. The embodied *electrical* energy is the product of the embodied *primary* energy and the grid efficiency η_{grid}. Throughout this study, we assume $\eta_{grid} = 0.30$ (consistent with ref. 24).

¶ The $ESOI_e$ ratio is identical in definition to the *net external energy ratio* (NEER).[25] The same quantity has also been described as the *energy return factor*.[26]

‖ We make the simplifying assumption that the electrolyzer and fuel cell are always operated at their nameplate power.

** The lower heating value energy content of hydrogen (120.21 MJ kg^{-1} = 33.4 kW h kg^{-1}).

we define the energy-to-power ratio

$$R = \frac{S}{P_{FC}} \tag{10}$$

which has units of time. For a RHFC system, the maximum dispatch duration is given by $R \times \eta_{FC}$.

To parametrize eqn (9) in terms of R, we first note that the energy content of the hydrogen produced by the electrolyzer over the system lifetime ($=\eta_{lyz}T_{lyz}P_{lyz}$) is equal to the energy content of the hydrogen consumed during the system lifetime $\left(=\frac{1}{\eta_{FC}}T_{FC}P_{FC}\right)$. We therefore assume in the following analysis that the power capacities and operating durations of the system satisfy the relation

$$\eta_{lyz}T_{lyz}P_{lyz} = \frac{1}{\eta_{FC}}T_{FC}P_{FC} \tag{11}$$

or, equivalently,

$$\eta_{lyz}\eta_{FC}T_{lyz}P_{lyz} = T_{FC}P_{FC} \tag{12}$$

Substituting this expression into eqn (9) yields

$$ESOI_e = \frac{1}{\frac{1}{\eta_{lyz}\eta_{FC}T_{lyz}}\left(\left[\frac{T_{lyz}}{\tau_{lyz,stack}}\right]\zeta_{lyz,stack} + \zeta_{lyz,BOS} + \zeta_{comp}\right) + \frac{1}{T_{FC}}\left(R\varepsilon_{st} + \left[\frac{T_{FC}}{\tau_{FC,stack}}\right]\zeta_{FC,stack} + \zeta_{FC,BOS}\right)} \tag{13}$$

(See ESI† for full derivation.)

2.1.3 Round-trip efficiency. The lifetime round-trip efficiency of the RHFC system is

$$\eta_{system} = \frac{E_{out}^{life}}{E_{in}^{life}} \tag{14}$$

where E_{in}^{life} is the energy that flows into the RHFC during its operation. There are two contributions to E_{in}^{life}: the energy that flows directly into the electrolyzer for storage, and the energy required for hydrogen compression.

$$\eta_{system} = \frac{E_{out}^{life}}{E_{op,lyz} + E_{op,comp}} \tag{15}$$

The lifetime energy input into the electrolyzer, $E_{op,lyz}$, is the product of the electrolyzer's cumulative operating duration and power capacity.

$$E_{op,lyz} = T_{lyz}P_{lyz} \tag{16}$$

The lifetime energy output is the product of the fuel cell's cumulative operating duration and power (eqn (4)).

We determine the lifetime energy requirement for hydrogen compression relative to the energy content of the hydrogen produced in the system. For this, we use the compression efficiency η_{comp}, *i.e.* the proportion of the energy content available from a quantity of hydrogen after subtracting the energy required to compress it.

$$E_{op,comp} = E_{H_2}^{life}\left(\frac{1}{\eta_{comp}} - 1\right) \tag{17}$$

where $E_{H_2}^{life}$ is the energy content of all the hydrogen produced (and consumed) within the RHFC system during its lifetime. This is equal to the energy output (as hydrogen) from the electrolyzer:

$$E_{H_2}^{life} = \eta_{lyz}T_{lyz}P_{lyz} \tag{18}$$

Substituting into eqn (17) yields

$$E_{op,comp} = \eta_{lyz}T_{lyz}P_{lyz}\left(\frac{1}{\eta_{comp}} - 1\right) \tag{19}$$

Substituting eqn (4), (16), and (19) into (15) and collecting terms yields

$$\eta_{system} = \frac{T_{FC}P_{FC}}{T_{lyz}P_{lyz}\left[1 + \eta_{lyz}\left(\frac{1}{\eta_{comp}} - 1\right)\right]} \tag{20}$$

Finally, we can substitute eqn (12) and cancel terms to obtain

$$\eta_{system} = \frac{\eta_{lyz}\eta_{FC}}{1 + \eta_{lyz}\left(\frac{1}{\eta_{comp}} - 1\right)} \tag{21}$$

2.2 Reference case values

The technical operating characteristics of the reference case RHFC system (Table 1) were compiled from the literature. We have converted all physical quantities to SI units.

2.2.1 Alkaline water electrolyzer. Alkaline water electrolyzers are a mature technology with lifetimes of 100 000 h ($\tau_{lyz} = 3.6 \times 10^8$ s), and system efficiencies of $\eta_{lyz} = 0.7$.†† [27,28]

To determine the energy intensity of alkaline water electrolyzers (AWE's), life cycle inventory (LCI) data are required. Unfortunately, no peer-reviewed LCI's are available for alkaline water electrolyzers. However, an empirical LCI is available for an alkaline fuel cell (AFC), a 2010 study by Staffell and Ingram (Table S1, ESI†).[39] Although AWE's and AFC's are designed differently, both employ nickel as a catalyst, at the anode of an AFC and the cathode of an AWE.[27,39–41] We judge that because of the partial overlap in this key energy-intense material, the AFC LCI provides a useful approximation when estimating the embodied energy of the AWE. From this life-cycle inventory and Ecoinvent data,[42] we determined a final value of 1.36×10^6 $(MJ)_{prim}/(MW)_{el}$ for the cell stack of the alkaline fuel cell model analyzed by Staffell and Ingram. To convert from primary to electrical energy, we multiply by $\eta_{grid} = 0.30$ to obtain a final value of $\zeta_{lyz,stack} = 4.1 \times 10^5$ $(MJ)_{el}/(MW)_{el}$.

This approach necessarily introduces significant uncertainty into our estimate of $\zeta_{lyz,stack}$, and we examine a wide range of values in our sensitivity analysis (Section 3.2).

†† We make the simplifying assumption that the electrolyzer and fuel cell are always operated at their nameplate power, with their nameplate efficiency. In real fuel cells, the system efficiency decreases with power output.

Table 1 Reference case values for the operating parameters of a regenerative hydrogen fuel cell

Component	Symbol	Quantity	Value		Note	Ref.
Alkaline electrolyzer	T_{lyz}	Total electrolyzer operating time	3.6×10^8	s	$= 1.0 \times 10^5$ h	—[a]
	P_{lyz}	Electrolyzer power	5	MW		—[a]
	η_{lyz}	Electrolyzer system efficiency[b,e]	0.7	—		27 and 28
	τ_{lyz}	Lifetime of electrolyzer stack	3.6×10^8	s	$= 1.0 \times 10^5$ h	29
	$\zeta_{lyz,stack}$	Energy intensity of electrolyzer stack	4.1×10^5	MJ $(MW)^{-1}$		—[c]
	$\zeta_{lyz,BOS}$	Energy intensity of electrolyzer BOS	3.3×10^5	MJ $(MW)^{-1}$		—[d]
Hydrogen storage and compression	η_{comp}	Efficiency of hydrogen compression	0.89	—		30
	ζ_{comp}	Energy intensity of hydrogen compression	6.5×10^4	MJ $(MW)^{-1}$		31
	S	Hydrogen storage capacity	3.0×10^5	MJ	= 84 MW h	—[a]
	ε_{st}	Energy intensity of storage[e]	8.0	MJ $(MW)^{-1}$	= 2900 MJ $(MW\ h)^{-1}$	32 and 33
PEM fuel cell	T_{FC}	Total fuel cell operating time	2.3×10^8	s	$= 6.4 \times 10^4$ h	—[a]
	P_{FC}	Fuel cell power	2.6	MW		—[a]
	η_{FC}	Fuel cell system efficiency[b,e]	0.47	—		28
	τ_{FC}	Lifetime of fuel cell stack	3.6×10^7	s	$= 1.0 \times 10^4$ h	34
	$\zeta_{FC,stack}$	Energy intensity of fuel cell stack	1.7×10^5	MJ $(MW)^{-1}$		35–38[f]
	$\zeta_{FC,BOS}$	Energy intensity of fuel cell BOS	1.7×10^5	MJ $(MW)^{-1}$		31
Full system	η_{system}	System efficiency	0.30	—		—[g]
	R	Energy-to-power ratio	1.2×10^5	s	= 32 h	—[h]

[a] The value of this parameter is chosen by the project designers, and does not depend on technology status. [b] System energy efficiency is defined as the energy in the hydrogen produced by the system (on a LHV basis) divided by the sum of the feedstock energy (LHV) plus all other energy used in the process. [c] See Section 2.2.1. [d] See Section 2.2.1. [e] LHV basis. [f] See Table S3 (ESI). [g] See Section 2.1.3. [h] $R = S/P_{FC}$.

To estimate the electrolyzer balance-of-system (BOS) energy intensity, we consider a commercial 2.2 MW electrolyzer produced by NEL hydrogen. The frame and ancillary systems of this electrolyzer weigh 60 000 kg.[31] They are fabricated mostly of steel, so we approximate the entire mass as consisting of steel. Using an embodied energy value for steel of 40.0 MJ kg^{-1},[33] this quantity of steel has an embodied energy of 2.4×10^6 $(MJ)_{prim}$, corresponding to an energy intensity of 1.1×10^6 $(MJ)_{prim}/(MW)_{el}$ or $\zeta_{lyz,BOS} = 3.3 \times 10^5$ $(MJ)_{el}/(MW)_{el}$.

2.2.2 Hydrogen compression and storage. Adiabatic compression of hydrogen from ambient pressure to 20 MPa requires approximately 14.4 MJ kg^{-1}.[32] This is 12% of the energy content of the hydrogen being compressed (LHV basis), resulting in an efficiency of $\frac{1}{1+0.12}$ or $\eta_{comp} = 0.89$.

To determine the energy intensity of a hydrogen compressor, we consider a representative commercially available compressor (RIX Industries model 4VX-S).[43] This compressor has a capacity of 48 N m^3 h^{-1} (30 SCFM), which is approximately the output of a 240 kW electrolyzer, and weighs 1300 kg (3000 pounds). Since the compressor is fabricated predominantly of steel, we approximate its materials inventory as 100% steel. Using an embodied energy value for steel of 40.0 $(MJ)_{prim}$ kg^{-1},[33] this corresponds to an embodied energy of 5.5×10^4 $(MJ)_{prim}$. As the electrolyzer power capacity determines the hydrogen flow rate, which in turn determines the capacity required of the compressor, we normalize the energy intensity of the compressor to the power capacity of the electrolyzer. For the compressor described here, this gives an energy intensity of 2.3×10^5 $(MJ)_{prim}/(MW)_{el}$, or $\zeta_{comp} = 6.5 \times 10^4$ $(MJ)_{el}/(MW)_{el}$.

To estimate the energy intensity of compressed hydrogen storage, we considered a 58 kg steel cylinder that holds 0.72 kg of hydrogen at 20 MPa.[32] To restate this mass of steel in terms of energy, we use the same value for the energy intensity of steel as the previous calculation – 40.0 $(MJ)_{prim}$ kg^{-1} – and assume that the tank is made entirely of steel. To restate this mass of hydrogen as a quantity of energy, we consider the energy content of hydrogen of 120.2 MJ kg^{-1} (LHV basis). The steel cylinder described here then has an energy intensity for hydrogen storage of 26.8 $(MJ)_{prim}/(MJ)_{LHV}$. We multiply by $\eta_{grid} = 0.30$ to obtain a final value of $\varepsilon_{st} = 8.0$ $(MJ)_{el}/(MJ)_{LHV}$.

2.2.3 PEM fuel cell. For fuel cell efficiency, we adopt the value of $\eta_{FC} = 0.47$ reported in 2013 by Verhage *et al.* for a 72 kW stationary PEM fuel cell power plant.[44]

We assume a fuel cell stack lifetime of 10 000 h ($\tau_{FC} = 3.6 \times 10^7$), which is a lower bound for commercially available PEM fuel cell stacks.[44,45] For the energy intensity of the PEM fuel cell stack, we critically reviewed the PEMFC life-cycle analysis literature to determine a value of 5.7×10^5 $(MJ)_{prim}/MW_{el}$ (see ESI†). To convert from primary to electrical energy, we multiply by $\eta_{grid} = 0.30$ to obtain $\zeta_{FC,stack} = 1.7 \times 10^5$ $(MJ)_{el}/(MW)_{el}$. For the energy intensity of the fuel cell balance of system, we add the same value, or $\zeta_{FC,BOS} = 1.7 \times 10^5$ $(MJ)_{el}/(MW)_{el}$.‡‡

2.3 $ESOI_e$ ratios of batteries and geological storage

The expression to determine the $ESOI_e$ ratio of a battery is simpler than for a RHFC, since a battery does not contain separate power and energy components. We treat energy storage in pumped hydro and compressed air/natural gas in the same way as for batteries. In addition, we revise the previously reported $ESOI_e$ ratios for these technologies, introduced by

‡‡ Available analyses estimate the balance-of-system contribution to total PEMFC energy intensity at 9% and 56% in systems that do not include a natural gas reformer (Table S2, ESI†).

Table 2 Characteristics and $ESOI_e$ ratios of battery and geologic storage technologies

	λ	D	ε_e	$ESOI_e$
LIB	6000	80	136	35
NaS	4750	80	146	26
VRB	2900	100	208	14
ZnBr	2750	80	151	15
PbA	700	80	96	5.8
CAES	25 000	100	22	1100
PHS	25 000	100	30	830

Barnhart and Benson,[46] to reflect a true cradle-to-gate assessment.§§ The $ESOI_e$ ratio for batteries and geologic storage is calculated as

$$ESOI_e = \frac{\lambda D}{\varepsilon_e} \quad (22)$$

where λ is the cycle life of the device; D is the depth of discharge; and ε_e is the cradle-to-gate electrical embodied energy. The technology characteristics and $ESOI_e$ ratios for several storage technologies are collected in Table 2. These technologies include lithium ion (LIB), sodium sulfur (NaS), vanadium (VRB), zinc bromine (ZnBr), and lead acid (PbA) batteries; compressed air energy storage (CAES); and pumped hydro storage (PHS).

3 Results

3.1 $ESOI_e$ ratio of a regenerative hydrogen fuel cell

Our reference case RHFC system is for a hypothetical wind farm producing P_{lyz} = 5 MW of overgeneration for eight hours per day. We set the cumulative operating duration of the electrolyzer equal to the lifetime of the electrolyzer stack, or $T_{lyz} = \tau_{lyz,stack} = 3.6 \times 10^8$ s (100 000 h). At eight hours per day of operation, this corresponds to a thirty-four year service life. The system has enough compressed hydrogen storage capacity to store all the excess energy generated over three days (*i.e.* 24 hours of operation), which is 3.02×10^5 MJ at η_{lyz} = 0.7 (equal to 84 MW h or 251 kg H_2 [LHV basis]). In order for the system to provide continuous power for five hours (a suitable duration for load leveling of renewables[9]) from a single day's generation, the fuel cell power rating is set to P_{FC} = 2.6 MW. This corresponds (from eqn (11)) to a lifetime fuel cell operating duration of $T_{FC} = 2.3 \times 10^8$ s (64 000 h). From eqn (21), the reference case RHFC system has a round-trip efficiency of η_{system} = 0.30.

A RHFC energy storage facility with these technical characteristics and configuration has an $ESOI_e$ ratio of 59 (from eqn (9)). This is higher than lithium ion batteries ($ESOI_e$ = 35), and much lower than pumped hydro ($ESOI_e$ = 830) and compressed air/natural gas ($ESOI_e$ = 1100).

§§ In ref. 46 this ratio is calculated as $ESOI = \frac{\lambda \eta D}{\varepsilon}$, where η is the dimensionless round-trip efficiency of the storage device. However, because battery storage capacities are quoted as discharge capacities, η should be omitted from this expression in order to accurately quantify the lifetime energy output. See Section 4.1.1 for discussion of including use-phase energy costs of inefficiency in energy return ratios. Note that the rank ordering of technologies by $ESOI_e$ value, calculated using the revised equation (*i.e.* (22)) (Table 2), is almost unchanged from the previously reported order in ref. 46.

3.2 $ESOI_e$ sensitivity analysis

A univariate sensitivity analysis, using the base parameters in Table 1, shows that the $ESOI_e$ ratio of the RHFC system is strongly influenced by the efficiency, lifetime, and energy intensity of the fuel cell stack (Fig. 3 and Table 3). For instance, doubling the fuel cell stack lifetime would increase the $ESOI_e$ ratio to 68. The same increase in the $ESOI_e$ ratio would result from increasing the fuel cell efficiency from 47% to 57%, or reducing the fuel cell stack energy intensity from 1.7×10^5 to 1.1×10^5 $(MJ)_{el}/(MW)_{el}$.

The energy-to-power ratio R also strongly affects the system's net energy performance. This parameter is directly proportional to the discharge time of the fully-charged RHFC, a key operational consideration for energy storage facilities. The discharge time is given by $R \times \eta_{FC}$. The net energy benefit of a RHFC system is maximized with an R value under $1 \times 10^{4.5}$ s (8.8 h, providing up to 4 h of dispatchable power from the fully charged state with η_{FC} = 0.47). However, the $ESOI_e$ ratio diminishes dramatically as R increases beyond this value (Fig. 3).

The $ESOI_e$ ratio is moderately sensitive to the energy intensity of the compressed hydrogen storage, the energy intensity of the electrolyzer balance of system, and the efficiency of the electrolyzer. The energy intensity of the electrolyzer stack, whose value is the most uncertain among all the technical parameters (Section 2.2.1), is also a moderately sensitive parameter. The energy intensity of the fuel cell balance of system has almost no influence on the $ESOI_e$ ratio.

The energy-to-power ratio R has an important interaction with the technical performance parameters such as lifetime and energy intensity of the fuel cell. At small values of R, technology advances such as improvements in fuel cell lifetime and efficiency can significantly increase the $ESOI_e$ ratio of the RHFC system. However, larger values of R (providing longer dispatch duration from a single charge) diminish the impact of technology improvements on the $ESOI_e$ ratio (Fig. 4).

3.3 Net energy analysis of hydrogen storage *versus* curtailment for renewables overgeneration

Grid-scale energy storage can avoid wasteful curtailment and allow greater total energy output from an intermittent generation facility. However, constructing the energy storage requires an energy input. Net energy analysis can determine when the energy benefit of avoiding curtailment outweighs the energy cost of building new storage capacity.[24]

We consider a generating facility that experiences overgeneration, and we wish to determine whether installing energy storage will provide a net energy benefit over curtailment. The generating facility itself has an energy return on investment of $[EROI]_{gen}$. Due to overgeneration, a fraction ϕ of the generated power must be diverted away from transmission. This diverted power may be stored for later use, or curtailed and lost (Fig. 5).

When generation is curtailed (and not stored), the EROI of the generation source decreases to

$$[EROI]_{curt} = (1 - \phi)[EROI]_{gen} \quad (23)$$

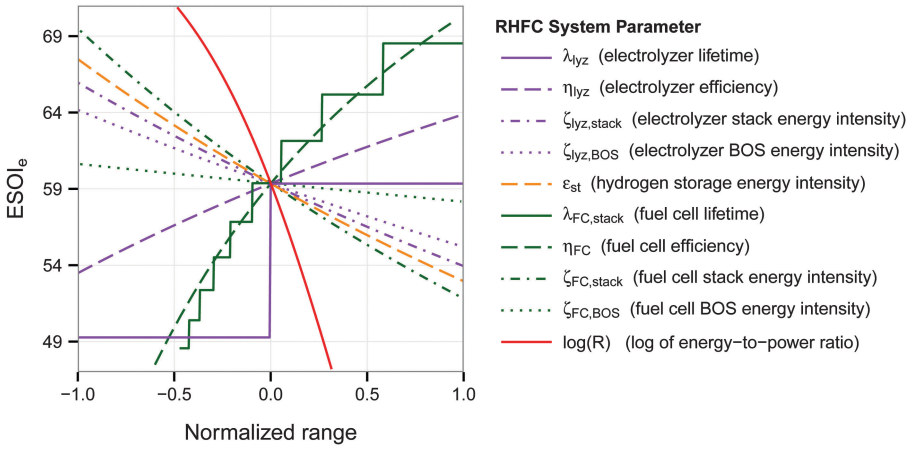

Fig. 3 Dependence of $ESOI_e$ ratio on individual system parameters. Calculated from eqn (9). The range of each parameter is specified in Table 3.

Table 3 Range of each parameter in the univariate sensitivity analysis (Fig. 3)

Parameter	Low value (−1.0)	Reference value (0.0)	High value (1.0)
η_{lyz}	0.55	0.70	0.85
$\zeta_{lyz,stack}$	2.1×10^5 MJ MW^{-1}	4.1×10^5 MJ MW^{-1}	6.1×10^5 MJ MW^{-1}
$\zeta_{lyz,BOS}$	2.0×10^5 MJ MW^{-1}	3.3×10^5 MJ MW^{-1}	5.0×10^5 MJ MW^{-1}
τ_{lyz}	1.8×10^8 s (50 000 h)	3.6×10^8 s (100 000 h)	5.4×10^8 s (150 000 h)
η_{st}	0.82	0.89	0.96
ε_{st}	4.0 MJ MJ^{-1}	8.0 MJ MJ^{-1}	12.0 MJ MJ^{-1}
η_{FC}	0.22	0.47	0.72
$\zeta_{FC,stack}$	9.0×10^4 MJ MW^{-1}	1.7×10^5 MJ MW^{-1}	2.5×10^5 MJ MW^{-1}
$\zeta_{FC,BOS}$	9.0×10^4 MJ MW^{-1}	1.7×10^5 MJ MW^{-1}	2.5×10^5 MJ MW^{-1}
τ_{FC}	0 s (0 h)	3.6×10^7 s (10 000 h)	7.2×10^7 s (20 000 h)
log(R)	4.1	5.1	6.1

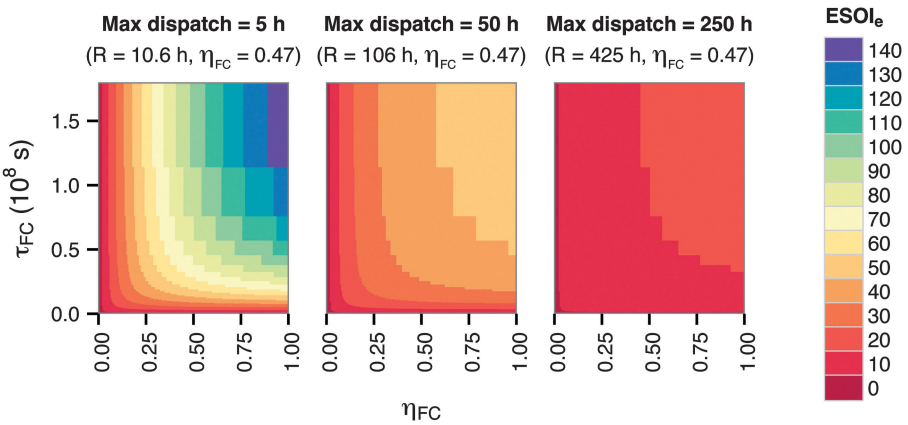

Fig. 4 Dependence of $ESOI_e$ ratio on τ_{FC}, η_{FC}, and R. Calculated from eqn (9).

If the overgeneration is instead diverted to storage in a local mini-grid, the aggregate EROI of the storage-equipped mini-grid is

$$[\mathrm{EROI}]_{grid} = \frac{1 - \phi + \eta_{st}\phi}{\frac{1}{[\mathrm{EROI}]_{gen}} + \frac{\phi}{\mathrm{ESOI}_e}} \quad (24)$$

(See ESI† for derivation.)

Both $[\mathrm{EROI}]_{curt}$ and $[\mathrm{EROI}]_{grid}$ are always less than $[\mathrm{EROI}]_{gen}$. However, $[\mathrm{EROI}]_{grid}$ may be greater or less than $[\mathrm{EROI}]_{curt}$, depending on the characteristics of the storage technology used. The choice of whether to build storage or accept curtailment therefore depends on the $ESOI_e$ ratio, as well as on the efficiency of the storage facility, the EROI of the generation technology, and the expected diversion ratio ϕ (eqn (24)).

The decision of whether to store or curtail depends on which quantity is greater, $[\mathrm{EROI}]_{curt}$ or $[\mathrm{EROI}]_{grid}$. By scaling this difference to $[\mathrm{EROI}]_{gen}$, we can quantify the benefit of storage, relative to curtailment, across different generating technologies with

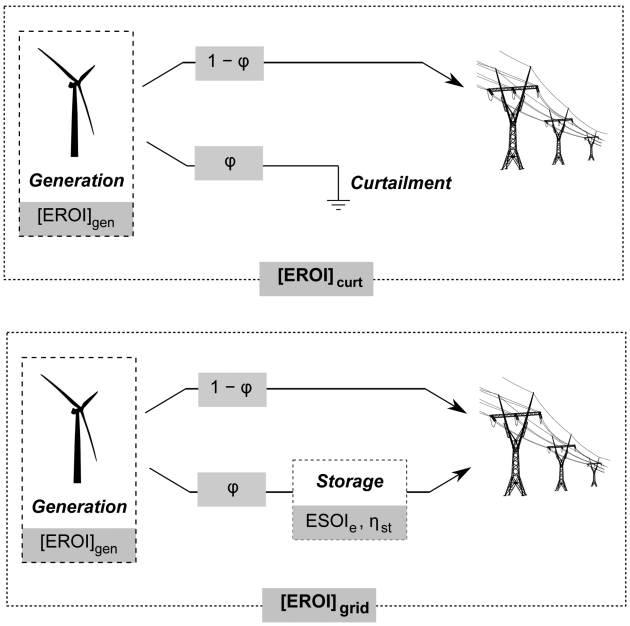

Fig. 5 A generating facility with $[EROI]_{gen}$ may experience curtailment, resulting in an overall EROI of $[EROI]_{curt}$. Alternatively, the overgeneration may be routed through a storage facility, resulting in an overall EROI of $[EROI]_{grid}$.

different values of $[EROI]_{gen}$.

$$\%\ \text{change in EROI} = \frac{[EROI]_{grid} - [EROI]_{curt}}{[EROI]_{curt}} \times 100 \qquad (25)$$

When this quantity is positive, building new energy storage capacity will yield a greater overall return on the energy invested in building the entire grid. When this quantity is negative, curtailing the overgeneration will yield a greater overall return on the energy investment, because the energy cost of building the storage facility outweighs the benefit of storing the energy for deferred use.

Because $[EROI]_{grid}$ is a function of the $ESOI_e$ ratio, and the $ESOI_e$ ratio of a RHFC system is in turn a function of the energy-to-power ratio R, the relative benefit of storing overgeneration in a RHFC system depends on the energy-to-power ratio of the RHFC system (Fig. 6).

For RHFC systems with low values of R, storing overgeneration from a photovoltaic system provides a net energy benefit over curtailing when the diversion ratio is above approximately 10%. At R values above 100 h (providing 47 h of continuous dispatch in our reference system), RHFC storage becomes break-even at intermediate diversion ratios, yielding neither an energy cost nor an energy benefit compared to curtailment. However, for power from wind farms, RHFC storage is unfavorable except at high diversion ratios ($\phi > 0.75$).

Barnhart *et al.* recently examined the net energy impacts of building storage *versus* accepting curtailment for a variety of geologic and battery storage technologies coupled with wind turbines and photovoltaic panels.[24] These included pumped hydro (PHS) and compressed air (CAES) as well as lithium ion (LIB),

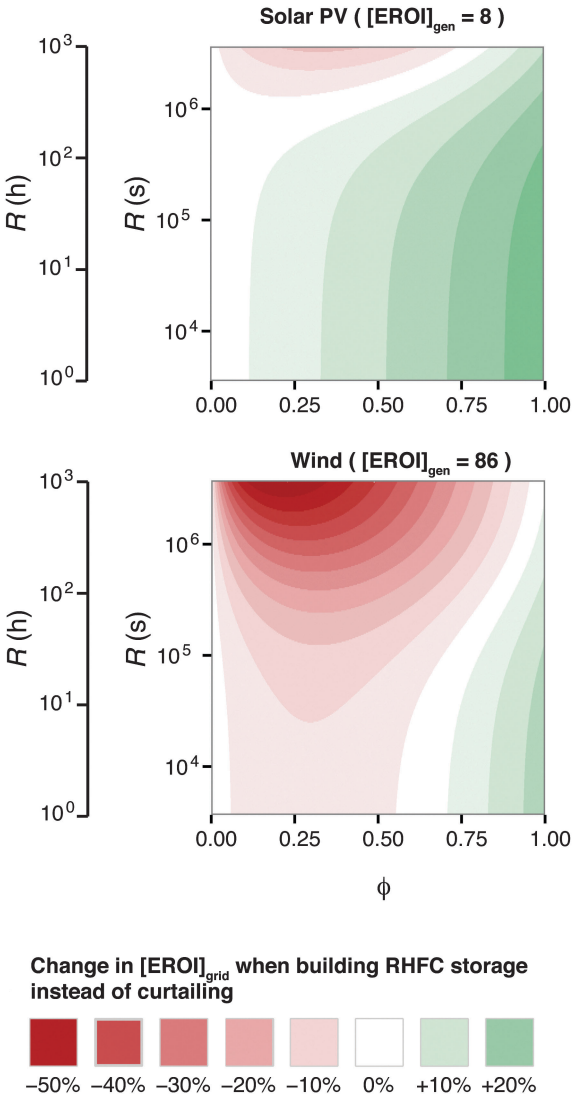

Fig. 6 Energy cost/benefit analysis of building the reference case hydrogen energy storage system to store overgeneration instead of curtailing it. Calculated from eqn (25).

sodium sulfur (NaS), vanadium (VRB), zinc bromine (ZnBr), and lead acid (PbA) batteries. Here, we extend this analysis with the corresponding results for a RHFC system (Fig. 7). The RHFC system analyzed for this comparison is identical to the reference system (Table 1) except that it contains 22 MW h (8.0×10^4 MJ) of hydrogen storage capacity, which provides four hours of discharge ($R = 8.5$ h). The maximum dispatch time assumed in this analysis varies for each technology, and is specified in the legend of Fig. 7.¶¶

For wind overgeneration, building the reference case RHFC system results in a $[EROI]_{grid}$ equal to the corresponding result for a building a LIB storage system, and more favorable than for other battery technologies. However, the $[EROI]_{grid}$ for any

¶¶ These durations were specified in the original data sources used in the analysis by Barnhart *et al.*,[7,46,47] except for LIB. The value of 2 h for LIB is characteristic of existing LIB energy storage installations.[48]

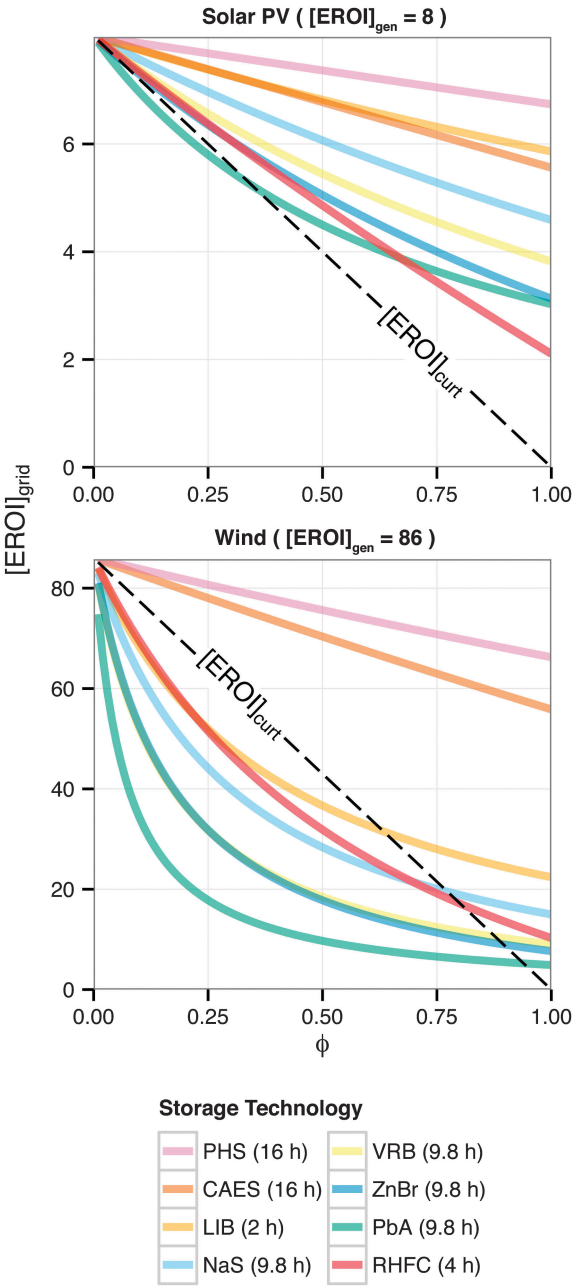

Fig. 7 Energy cost/benefit analysis of storing energy using different storage technologies. Calculated from eqn (24). Adapted from ref. 24.

non-geological storage option is lower than $[EROI]_{curt}$ for $\phi < 0.50$. In contrast, for photovolatic overgeneration, RHFC storage is less favorable than LIB or NaS, but preferable to curtailing.

4 Discussion

The present analysis evaluates the net energy balance of a discrete regenerative hydrogen fuel cell system containing an alkaline water electrolyzer and a PEM fuel cell. In this section, we compare RHFC's to LIB systems using two different measures of net energy benefit. We also examine the importance of

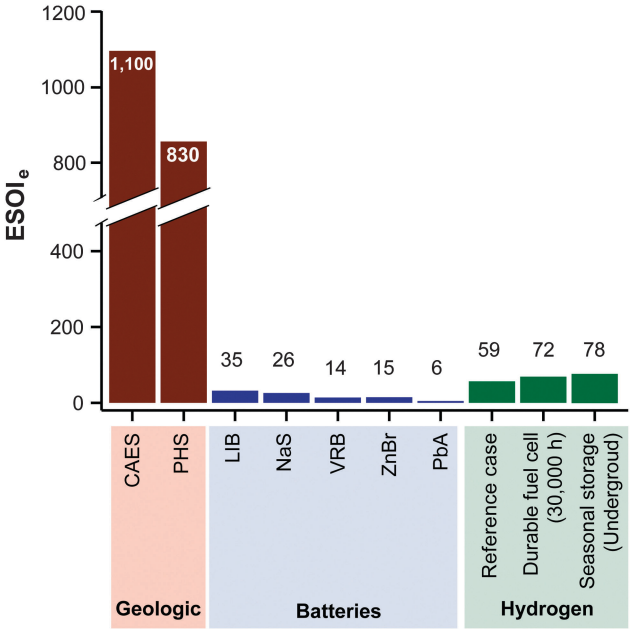

Fig. 8 $ESOI_e$ ratios of energy storage in geologic, battery, and regenerative fuel cell systems. (Values for geologic and battery technologies are taken from ref. 46.)

the materials in the contrast between the $ESOI_e$ ratios of these two technologies. We summarize the implications for fuel cell research and storage system design.

4.1 Comparison of RHFC and LIB energy storage systems

4.1.1 Embodied energy, system efficiency, and net energy indicators. Two distinct energy return ratios are useful in comparing different energy storage technologies. The first is the $ESOI_e$ ratio, which indicates how efficiently a storage system leverages energy inputs that are external to the energy storage process.‖ These energy inputs occur during the manufacturing phase of the storage system's life cycle, for preparing materials and assembling the system. The $ESOI_e$ ratio is primarily influenced by the quantity and energy intensity of the materials required for a particular storage system. It can have any positive value.

Lithium ion batteries (LIB's) have the highest $ESOI_e$ ratio (35) among a series of battery technologies being installed for grid storage (Fig. 8).[46] Energy storage in hydrogen, using the reference case RHFC system, has a $ESOI_e$ ratio of 59. This indicates that one joule of energy invested in manufacturing a RHFC system enables more output from energy storage than a joule invested in manufacturing a LIB system.

The round-trip efficiency of a storage system is a characteristic of the system's operation, rather than its manufacture, and is not reflected in the $ESOI_e$ ratio. It is accounted for in a second energy return ratio, the *overall energy efficiency* (η^*).[26] The overall energy efficiency compares the net energy output from the system to the total energy inputs. These total energy inputs include the energy directed into the system for storage

‖ The $ESOI_e$ ratio is identical in definition to the *net external energy ratio* (NEER).[25] The same quantity has also been described as the *energy return factor*.[26]

Table 4 $ESOI_e$ ratios for different RHFC system scenarios

Scenario	Description	$ESOI_e$
Reference case	(See Table 1)	59
Efficient fuel cell	$\eta_{FC} = 0.70$	78
Low-Pt fuel cell	Fuel cell Pt loading reduced by 50%	64
Composite cylinders	Compressed hydrogen vessel constructed of epoxy-polyacronitrile resin	69
Durable fuel cell	$\tau_{FC} = 30\,000$ h	72
Durable fuel cell with composite cylinders	$\tau_{FC} = 30\,000$ h, and compressed hydrogen vessel constructed of epoxy-polyacronitrile resin	102
Four months of storage	Hydrogen storage capacity adequate for four months of generation	4.0
Four months of storage with composite cylinders	Hydrogen storage capacity adequate for four months of generation, in vessel constructed of epoxy-polyacronitrile resin	9.2
Four months of storage in underground salt cavern	Hydrogen storage capacity adequate for four months of generation, in an underground salt cavern similar to compressed air storage caverns	78

during its operational life (E_{in}^{life}), as well as the manufacturing-phase external energy inputs (E_{emb}^{life}).

$$\eta^* = \frac{E_{out}^{life}}{E_{emb}^{life} + E_{in}^{life}} \quad (26)$$

The value of η^* for a storage system is strongly influenced by the system's round-trip efficiency, rather than by its materials requirements. Because $E_{out}^{life} < E_{in}^{life}$, η^* always lies between zero and unity. For the RHFC system, the embodied energy is negligible compared to the energy inputs during operation, so η^* for the RHFC system is approximately equal to its round-trip efficiency of 0.30. For the LIB, the embodied energy is small compared to the energy inputs during operation, but is not negligible, so the LIB's η^* of 0.83 is close to, but slightly lower than, its round-trip efficiency of 0.9.

These two different energy return ratios quantify two different dimensions of energy performance. The higher $ESOI_e$ ratio of the reference case RHFC system reflects its more efficient use of manufacturing energy to dispatch the same unit of electrical energy from storage. The LIB's higher overall energy efficiency (η^*) reflects its greater efficiency in handling the energy stored in the system during its operational life.

4.1.2 $ESOI_e$ ratio and system lifetime. Lifetime is an important consideration for energy storage systems. We can make a meaningful comparison between the lifetimes of RHFC and LIB systems by considering the total duration of discharge provided by each system as initially installed (excluding any component replacements). For LIB systems, we first consider the system's cycle life. A benchmark cycle life for a LIB system operating at 80% depth of charge is 6000 cycles.[47] We next consider the desired duration of discharge from a single cycle, which is five to ten hours for storing off-peak renewable power.[9] A LIB system with a 6000-cycle life, configured for five hours of discharge per cycle (the same as our reference case RHFC system), will provide 30 000 h of dispatchable power over its lifetime.***

The lifetime of a AWE–PEMFC RHFC system is limited by the fuel cell. A RHFC system identical to the reference case (Table 1), but with a fuel cell stack lifetime of 30 000 h (equal to the LIB lifetime discharge), has a $ESOI_e$ ratio of 72. (Ballard Power Systems presently advertises this cell stack lifetime for its stationary PEMFC systems.) Even with the more conservative PEMFC stack lifetime of 10 000 h used for the reference case, the $ESOI_e$ ratio of the RHFC system (59) exceeds that of the LIB system (35). A RHFC system with the same operational characteristics as a typical LIB system provides more energy dispatch for every joule of manufacturing energy input.

Table 5 Comparison of energy storage in RHFC and LIB systems using two different energy return ratios

	E_{out}^{life} (10^6 MJ)	E_{emb}^{life} (10^6 MJ)	E_{in}^{life} (10^6 MJ)	$ESOI_e$	η^*
RHFC[a]	592	9.92	1973	59	0.30
LIB[b]	677	64	752	35	0.83

[a] The reference case RHFC described in Table 1. [b] A LIB system with the characteristics in Table 2, and the same discharge capacity as the reference case RHFC system (39.5 MW h).

Although a longer PEMFC stack lifetime increases the $ESOI_e$ ratio, it has no effect on the overall energy efficiency of the system. This is because over the lifetime of the system, almost all the energy costs are due to efficiency losses, not to manufacturing the system (Table 5).

4.1.3 Energy-storing materials and embodied energy. Storing electricity in our reference case RHFC system has a more favorable $ESOI_e$ ratio than lithium ion batteries (Fig. 8). A detailed comparison of the functions of various materials included in these two storage devices provides some insight into this result. Each storage device includes certain materials that are directly involved in storing energy (as electric charge or compressed gas). Each device contains other materials that do not directly participate in energy storage, such as the materials in the electrolyzer and fuel cell of a RHFC system, and the current collectors in a battery.

Lithium ion batteries contain several materials that are directly involved in storing electric charge: a lithium intercalation compound at the cathode, highly reduced carbon at the anode, a lithium electrolyte, and a separator membrane.††† These four active charge-storing materials in a lithium ion battery account

*** This upper-bound value assumes ideal battery performance, and neglects the capacity decay that occurs in real battery systems.

††† The other materials in the battery perform other functions: *e.g.* copper and aluminum current collectors conduct charge (but do not store it); casing materials provide structural integrity.

for approximately 40% of the energy required to manufacture the battery (Table S6, ESI†).[49,50]

In a RHFC system using conventional cylinders to store compressed hydrogen gas, the only material directly involved in storing energy is the steel used to fabricate the cylinders. In our reference case RHFC system, the energy-storing material – the steel pressure vessel – accounts for only 26% of the embodied energy (Table S3, ESI†). In an otherwise identical RHFC system that uses composite cylinders for hydrogen storage (instead of more energy intensive steel cylinders), the storage component represents only 12% of the system's embodied energy. The materials that perform the intrinsic energy storage function in a LIB system are more energetically expensive than in an RHFC system, as a share of the total manufacturing energy costs.

This contrast is reflected by the different energy intensities of storing energy in compressed hydrogen storage *versus* lithium ion batteries. Estimates for the energy intensity of lithium ion battery storage range from 86 to 200 MJ MJ^{-1}.[47,49] This is several times our estimate of 28 MJ MJ^{-1} for compressed hydrogen storage in steel vessels.

4.2 Key technical parameters and implications for research

The most important technical parameters that influence the net energy balance of a RHFC system are the fuel cell efficiency, lifetime and energy intensity (Fig. 3). Extending the fuel cell lifetime beyond the reference value of 10 000 h would significantly increase the $ESOI_e$ ratio. For instance, increasing the lifetime to 30 000 h would increase the $ESOI_e$ ratio from 59 to 72 (Table 4). With a fuel cell stack lifetime of 50 000 h, and a fuel cell system efficiency of 0.60, the reference case RHFC system would have an $ESOI_e$ ratio of 110 (Fig. 4).

The energy intensity of the fuel cell is a moderately sensitive parameter (Fig. 3). Although the fuel cell energy intensity (2.1×10^5 MJ MW^{-1}) is less than our estimate of the electrolyzer energy intensity (5.1×10^5 MJ MW^{-1}), the short cell stack lifetime requires seven replacements of the fuel cell stack during the service lifetime of the RHFC system. Since the energy cost of the cell stack must be paid every time the stack is replaced, the fuel cell energy intensity is a higher-sensitivity parameter than the electrolyzer energy intensity, even though its absolute value is lower (1.7×10^5 *vs.* 4.1×10^5 MJ MW^{-1}). The fuel cell energy intensity is dominated by the energy cost of the platinum catalyst (40%) and carbon fiber (29%), followed by carbon paper (13%) and aluminum (12%) (Table S3, ESI†).

The significant research effort focused on reducing PEMFC catalyst loadings,[28,51] motivated primarily by cost considerations, is consistent with increasing the $ESOI_e$ ratio of a PEMFC-based RHFC system, since lower platinum loadings will reduce the energy intensity of the cell stack. However, because platinum accounts for less than half of the fuel cell's embodied energy (Table S3, ESI†), reduced platinum loadings will have only a modest impact on the $ESOI_e$ ratio of a AWE–PEMFC RHFC system. A 50% decrease in platinum loading yields only a 20% decrease in the fuel cell embodied energy, increasing the $ESOI_e$ ratio from 59 to 64.

Another relevant parameter is the energy intensity of the storage vessel. Our reference case RHFC system uses steel cylinders to store compressed hydrogen. However, lower energy intensities have been reported for compressed hydrogen storage in vessels made of aluminum (6.9 MJ MJ^{-1})[52] or reinforced epoxy (3.3 MJ MJ^{-1}).[53] Switching from a steel vessel to reinforced epoxy increases the system's $ESOI_e$ ratio from 59 to 69 (Table 4).

4.3 Energy-to-power ratio and implications for seasonal storage

The energy-to-power ratio R is directly proportional to the duration over which a storage system can continuously dispatch power from its fully charged state at maximum power (the maximum dispatch time is given by $R \times \eta_{FC}$). It is an important factor governing the net energy balance of a RHFC system (Fig. 3). The $ESOI_e$ ratio of storing energy in a RHFC system is greatest in systems with shorter continuous dispatch times (or, equivalently, systems that can store fewer hours of power intake). The design choices made when planning a RHFC storage facility can therefore make the difference between a system with excellent net energy balance and one that barely breaks even on the energy invested in its construction.

For instance, our reference case system, with an $ESOI_e$ ratio of 59, can store the energy from up to three days of overgeneration, providing up to 15 hours of continuous power. However, increasing the storage capacity to 90 h (for instance, to enhance load shifting capacity) would reduce the $ESOI_e$ ratio to 26. (On the other hand, if the storage capacity is reduced to only one day of overgeneration, the system $ESOI_e$ ratio would increase modestly to 69.)

Hydrogen storage has been proposed for seasonal energy storage to mitigate the seasonal variation in wind and solar generation.[8,21] A seasonal storage facility designed to store several months of generation would require a large energy-to-power ratio. When our reference scenario is modified to provide enough storage (in steel cylinders) for 120 days of generation, the energy cost of the increased storage capacity drives the $ESOI_e$ ratio down to 4.0.

This result shows that in order to provide a net energy benefit, a seasonal-scale RHFC system must use an alternative method for hydrogen storage. One possibility is underground salt caverns, as described by Crotogino *et al.*[54] and modeled by Maton *et al.*[55] We estimate an energy intensity of 3.0×10^{-7} MJ MJ^{-1} for storing hydrogen in subsurface caverns,‡‡‡ compared to 28 MJ MJ^{-1} for steel cylinders. This would result in an $ESOI_e$ ratio of 78 for a seasonal storage system,§§§ much more favorable than using above-ground hydrogen storage for seasonal load shifting. (However, this approach would constrain seasonal hydrogen storage to geologically suitable areas with nearby subsurface salt formations.)

Another possible approach is above-ground storage in large spherical pressurized tanks. Because of the smaller surface-area-to-volume ratio of large spheres, this storage geometry

‡‡‡ See ESI† for detailed calculation.

§§§ Similar to our reference case but with enough storage capacity to capture four months of generation.

would use less steel to store the same volume of gas, leading to a lower energy intensity of storage.

4.4 To store or curtail: RHFC's and storage technology alternatives

Energy storage is likely to have an important role in integrating intermittent renewable energy generation into the electric grid, including capturing overgeneration ("spilled power") for later use. The low round-trip efficiency of hydrogen storage suggests that building this type of storage will always result in a less favorable net energy outcome than other technology options with higher round-trip efficiencies. However, in some situations, its low round-trip efficiency is offset by its higher $ESOI_e$ ratio and a high energy return on investment (EROI) of the generating technology.

Constructing a new, dedicated RHFC system with a low energy-to-power ratio (less than 100 h) to store photovoltaic overgeneration provides a small net energy benefit (Fig. 6). The RHFC system has a low round-trip efficiency, which tends to make it less energetically favorable. However, this is offset by the low EROI of photovoltaic power (EROI = 8) – that is, it is energetically expensive to produce photovoltaic generating capacity (largely due to energy-intensive silicon refining).[46] Because more energy was invested to provide each kilowatt-hour of photovoltaic electricity, a photovoltaic-powered system can tolerate a lower storage efficiency and still realize a net energy benefit, when the storage capacity is efficiently utilized to capture overgeneration. However, the low round-trip efficiency of the RHFC system makes it a less favorable choice than lithium-ion (LIB) and sodium sulfur (NaS) batteries (Fig. 7). These battery technologies have lower $ESOI_e$ ratios (Fig. 8) but much higher round-trip efficiencies (90% for lithium ion; 80% for NaS[56]). (Pumped hydro and CAES storage are also more favorable than curtailment, but these storage options are site-limited.) It is preferable to store photovoltaic overgeneration in a RHFC system than to curtail, but it is even more preferable to store it in lithium ion or sodium sulfur batteries.

In contrast, constructing new, dedicated RHFC storage is generally unfavorable for wind overgeneration (Fig. 6): it is energetically preferable to simply curtail the wind overgeneration than to spend additional energy to build RHFC storage capacity. For wind power, at low diversion ratios ($\phi < 0.3$), the net energy impact of RHFC storage is similar to that of LIB storage (Fig. 7), even though LIB systems have a much higher round-trip efficiency.

It is noteworthy that even when the EROI of wind-generated electricity is reduced to $[EROI]_{grid}$ by storage in a hydrogen or LIB system, the resulting $[EROI]_{grid}$ is still higher than the EROI of fossil-generated electricity. For instance, if 25% of the output of a wind farm is diverted through the reference case RHFC system, the aggregate to $[EROI]_{grid}$ of the storage-equipped wind farm is approximately 50 (Fig. 7). (The result is the same if LIB is used to store the same fraction of output.) In contrast, combusting coal or natural gas provides electricity with an EROI of approximately 30.[57,58]

Net energy analysis describes the energy balance of these technologies, but it does not by itself guide or predict investment in one technology option over another. Technology cost and market structure are important considerations for modeling investment in or deployment of different technology options, and have been discussed elsewhere.[59–66]

4.5 Future work

The present analysis contains uncertainties which can be addressed by more complete life-cycle analysis data. The largest uncertainty is in the energy intensity value of the alkaline electrolyzer stack, which is a moderately sensitive parameter (Fig. 3). In addition, data on the balance-of-system contribution to energy intensity is lacking for alkaline electrolyzers, and limited for PEMFC's.

The present analysis makes the simplifying assumption that the electrolyzer and fuel cell operate at 100% of rated power. However, a more detailed model allowing variable operating power would more closely reflect actual systems, and could be coupled with overgeneration time series data to determine $ESOI_e$ ratios for RHFC operation under detailed variable-output scenarios.

While consideration of resource constraints is beyond the scope of the present analysis, the availability of platinum (or other precious metals) may impose a practical limit on the pace of installation of PEMFC-containing RHFC systems.

The AWE-PEMFC configuration examined in this analysis is only one of several possible technology configurations for implementing hydrogen storage in a RHFC system. PEMWE-PEMFC and AWE-ICE hydrogen storage systems are already in operation (Fig. 2). In addition, solid oxide electrolyzers and solid oxide fuel cells are a maturing technology class that may become attractive for use in RHFC systems. Further analysis is underway in our group to examine the net energy balance of these additional hydrogen storage technology configurations.

Finally, although the present analysis is restricted to systems that use hydrogen exclusively to produce electricity, there are several other possible uses for stored hydrogen. These include filling fuel cell vehicles, enriching the natural gas distribution system, local industrial consumption, and production of synthetic fuels. A flexible supply installation that can dispense hydrogen to multiple end uses may achieve a better net energy outcome than any single-use configuration. Net energy analysis of these other applications of grid-generated hydrogen, and of optimized flexible use, remains for future work.

5 Conclusion

Energy storage in hydrogen is a technically feasible option for grid-scale storage, and is already in pilot demonstrations. Because of its low round-trip efficiency, it may be overlooked in spite of its potential advantages, such as high energy density and low rate of self-discharge. In order to examine the potential benefits and drawbacks of hydrogen as a grid-scale energy storage technology, we apply net energy analysis to a representative hypothetical regenerative hydrogen fuel cell (RHFC) system.

We introduce and apply a method to determine the energy stored on invested ($ESOI_e$) ratio of a reference case RHFC system.

We find that the reference case RHFC system has a higher $ESOI_e$ ratio than lithium ion battery storage. This indicates that the hydrogen storage system makes more efficient use of manufacturing energy inputs to provide energy storage. One reason for this is that the steel used to fabricate a compressed hydrogen storage cylinder is less energetically costly, per unit of stored energy, than the materials that store electric charge in a battery (electrode paste, electrolyte, and separator). However, lithium ion batteries remain energetically preferable when considering the operation of the system, as well as its manufacture, due to their higher round-trip efficiency (90%). This is reflected in the overall energy efficiencies of the two storage technologies: the overall energy efficiency of a typical lithium ion battery system is 0.83, compared to 0.30 for the reference case RHFC system. This highlights that in spite of its relatively efficient use of manufacturing energy inputs, the round-trip efficiency of a RHFC system must increase before it can provide the same total energy benefit as other storage technologies. Higher RHFC round-trip efficiency relies on improved electrolyzer and fuel cell performance.

When storing overgeneration from wind turbines, energy storage in hydrogen provides an energy return similar to batteries, in spite of its lower round-trip efficiency. The aggregate EROI of wind generation augmented with RHFC storage is equal to that of the same wind facility augmented with lithium ion battery storage, when up to 25% of the electricity output passes through the storage system. For spilled power from solar photovoltaics, storage in hydrogen provides an EROI that is slightly higher than curtailment, though lower than batteries. As with other storage technologies, energy storage in hydrogen coupled to wind generation provides an overall EROI that is well above the EROI of fossil electricity generation.

Nomenclature

Abbreviations

AFC	Alkaline fuel cell
AWE	Alkaline water electrolyzer
BOS	Balance of system
CAES	Compressed air energy storage
CHP	Combined heat and power
EROI	Energy return on investment
ESOI	Energy stored on invested
ICE	Internal combustion engine
LHV	Lower heating value
LIB	Lithium ion battery
NaS	Sodium-sulfur
PbA	Lead acid
PEMFC	Polymer electrolyte membrane fuel cell
PEMWE	Polymer electrolyte membrane water electrolyzer
PHS	Pumped hydro storage
RHFC	Regenerative hydrogen fuel cell
VRB	Vanadium redox battery
ZnBr	Zinc bromine

Symbols

ε_e	Energy intensity of battery or geologic storage $[(MJ)_{electrical}/(MW)_{electrical}]$
ε_{st}	Energy intensity of hydrogen storage $[(MJ)_{electrical}/(MJ)_{LHV}]$
η^*	Overall energy efficiency [dimensionless]
η_{comp}	Efficiency of hydrogen compression [dimensionless]
η_{FC}	Fuel cell system efficiency [dimensionless]
η_{grid}	Grid efficiency of converting primary energy to electrical energy [dimensionless]
η_{lyz}	Electrolyzer system efficiency [dimensionless]
η_{system}	Overall efficiency of a storage system [dimensionless]
λ	Cycle life of a storage device [dimensionless]
τ_{FC}	Lifetime of fuel cell stack [s]
τ_{lyz}	Lifetime of electrolyzer stack [s]
ζ_{FC}	Energy intensity of fuel cell power $[(MJ)_{electrical}/(MW)_{electrical}]$
ζ_{lyz}	Energy intensity of electrolyzer power $[(MJ)_{electrical}/(MW)_{electrical}]$
D	Depth of discharge of a storage device [dimensionless]
$E^{life}_{emb,FC}$	Embodied energy in the fuel cell $[(MJ)_{electrical}]$
$E^{life}_{emb,lyz}$	Embodied energy in the electrolyzer $[(MJ)_{electrical}]$
$E^{life}_{emb,st}$	Embodied energy in the compressed hydrogen storage vessel $[(MJ)_{electrical}]$
E^{life}_{emb}	Embodied energy in the storage system $[(MJ)_{electrical}]$
E^{life}_{out}	Cumulative energy dispatched by a storage system throughout its lifetime $[(MJ)_{electrical}]$
$E^{life}_{H_2}$	Energy content of the hydrogen produced in the RHFC system throughout its lifetime $[(MJ)_{LHV}]$
$E_{op,comp}$	Energy consumed to operate the hydrogen compressor of a RHFC system $[(MJ)_{electrical}]$
$E_{op,lyz}$	Energy consumed by the electrolyzer during operation of a RHFC system $[(MJ)_{electrical}]$
P_{FC}	Fuel cell power $[(MW)_{electrical}]$
P_{lyz}	Electrolyzer power $[(MW)_{electrical}]$
R	Energy-to-power ratio of a storage system [s]
S	Hydrogen storage capacity $[(MJ)_{LHV}]$
T_{FC}	Cumulative fuel cell operating duration during RHFC service lifetime [s]
T_{lyz}	Cumulative electrolyzer operating duration during RHFC service lifetime [s]
$[EROI]_{curt}$	EROI of a storage-equipped generation facility when some generation is curtailed [dimensionless]
$[EROI]_{gen}$	EROI of a power generation facility [dimensionless]
$[EROI]_{grid}$	Aggregate EROI of a storage-equipped generation facility [dimensionless]
$ESOI_e$	Energy stored on invested ratio (electrical/electrical) $[(MJ)_{electrical}/(MW)_{electrical}]$

Acknowledgements

We thank Michael Carbajales-Dale (Clemson University); Michael Lepech and Mauro Pasta (Stanford University); Elena Krieger (PSE Healthy Energy); Li Zhao (National Fuel Cell Research Center); and Markus Felgenhauer (Technical University of Munich) for helpful discussions. This work was supported by the Global Climate and Energy Project at Stanford University. CJME would like to acknowledge support from Climate-KIC and the Grantham Institute for Climate Change through a PhD studentship.

References

1 International Energy Agency, IEA Statistics: Renewables Information, OECD/IEA, 2014.
2 U.S. Energy Information Administration, International Energy Statistics: Renewables Electricity Generation, http://www.eia.gov/countries/data.cfm.
3 M. Fischedik, R. Schaeffer, A. Adedoyin, M. Akai, T. Bruckner, L. Clarke, V. Krey, I. Savolainen, S. Teske, D. Urge-Vorsatz and R. Wright, in *IPCC Special Report on Renewable Energy Sources and Climate Change Mitigation*, ed. O. Edenhofer, R. Pichs-Madruga, Y. Sokona, K. Seyboth, P. Matschoss, S. Kadner, T. Zwickel, P. Eickemer, G. Hansen, S. Schlomer and C. von Stechow, Cambridge University Press, Cambridge, United Kingdom and New York, NY, USA, 2011, pp. 791–864.
4 R. Wiser and M. Bolinger, 2011 Wind Technologies Market Report, U.S. Department of Energy, 2012.
5 International Energy Agency, World Energy Outlook 2013, 2013.
6 M. Hand, S. Baldwin, E. DeMeo, J. Reilly, T. Mai, D. Arent, G. Porro, M. Meshek and D. Sandor, *Renewable Electricity Futures Study*, National Renewable Energy Laboratory, Golden, CO, 2012.
7 P. Denholm and M. Hand, *Energy Policy*, 2011, **39**, 1817–1830.
8 M. Beaudin, H. Zareipour, A. Schellenberglabe and W. Rosehart, *Energy Sustainable Dev.*, 2010, **14**, 302–314.
9 Electric Power Research Institute, Electric Energy Storage Technology Options: A White Paper Primer on Applications, Costs, and Benefits, Electric Power Research Institute Technical Report #1020676, 2010.
10 A. Evans, V. Strezov and T. J. Evans, *Renewable Sustainable Energy Rev.*, 2012, **16**, 4141–4147.
11 J. Divisek and B. Emonts, in *Handbook of Fuel Cells*, ed. W. Vielstich, A. Lamm, H. A. Gasteiger and H. Yokokawa, John Wiley & Sons, Ltd, Chichester, UK, 2010, ch. 1.
12 G. Gahleitner, *Int. J. Hydrogen Energy*, 2013, **38**, 2039–2061.
13 B. Kroposki, J. Levene and K. Harrison, Electrolysis: Information and Opportunities for Electric Power Utilities, National Renewable Energy Laboratory Technical Report NREL/TP-581-40605, 2006.
14 O. Z. Sharaf and M. F. Orhan, *Renewable Sustainable Energy Rev.*, 2014, **32**, 810–853.
15 S. Verhelst, *Int. J. Hydrogen Energy*, 2014, **39**, 1071–1085.
16 C. White, R. Steeper and A. Lutz, *Int. J. Hydrogen Energy*, 2006, **31**, 1292–1305.
17 J. Erjavic, *Hybrid, Electric and Fuel-Cell Vehicles*, Delmar/Cengage Learning, Inc., Clifton Park, NY, 2nd edn, 2013, ch. 11.
18 A. Veziroglu and R. Macario, *Int. J. Hydrogen Energy*, 2011, **36**, 25–43.
19 U. Eberle, B. Müller and R. von Helmolt, *Energy Environ. Sci.*, 2012, **5**, 8780.
20 D. U. Eberle and D. R. von Helmolt, *Energy Environ. Sci.*, 2010, **3**, 689.
21 J. Andrews and B. Shabani, *Int. J. Hydrogen Energy*, 2012, **37**, 6–18.
22 D. Steward, G. Saur, M. Penev and T. Ramsden, Lifecycle Cost Analysis of Hydrogen Versus Other Technologies for Electrical Energy Storage, National Renewable Energy Laboratory Technical Report NREL/TP-560-46719, 2009.
23 M. Carbajales-Dale, C. J. Barnhart, A. R. Brandt and S. M. Benson, *Nat. Clim. Change*, 2014, **4**, 524–527.
24 C. J. Barnhart, M. Dale, A. R. Brandt and S. M. Benson, *Energy Environ. Sci.*, 2013, **6**, 2804.
25 A. R. Brandt and M. Dale, *Energies*, 2011, **4**, 1211–1245.
26 C. J. Rydh and B. A. Sandén, *Energy Convers. Manage.*, 2005, **46**, 1980–2000.
27 D. Stolten and D. Krieg, in *Hydrogen and Fuel Cells*, ed. D. Stolten, Wiley-VCH Verlag GmbH, 2010, ch. 12.
28 U.S. DOE, Multi-Year Research, Development and Demonstration Plan, U.S. DOE, 2012, ch. 3.4.
29 I. Cerri, F. Lefebvre-Joud, P. Holtappels, K. Honegger, T. Stubos and P. Millet, *Scientific Assessment in support of the Materials Roadmap enabling Low Carbon Energy Technologies*, European Commission Joint Research Centre Institute for Energy and Transport, Petten, 2012.
30 B. Hobein and R. Kruger, in *Hydrogen and Fuel Cells – Fundamentals, Technologies, Applications*, ed. D. Stolten, Wiley-VCH Verlag GmbH & Co. KGaA, Weinheim, 2010, ch. 18.
31 H. Langlas, 2014, personal communication.
32 M. Hirscher and M. Klell, in *Handbook of Hydrogen Storage*, ed. M. Hirscher, Wiley-VCH Verlag GmbH & Co. KGaA, 2010, ch. 1.
33 M. Weiss, J. B. Heywood, E. M. Drake, A. Shafer and F. F. AuYeung, On the road in 2020: A life-cycle analysis of new automobile technologies, Massachusetts Institute of Technology Energy Laboratory Technical Report #MIT EL 00-003, 2000.
34 Y. Wang, K. S. Chen, J. Mishler, S. C. Cho and X. C. Adroher, *Appl. Energy*, 2011, **88**, 981–1007.
35 V. Karakoussis, M. Leach, R. van der Vorst, D. Hart, J. Lane, P. Pearson and J. Kilner, Environmental Emissions of SOFC and SPFC System Manufacture and Disposal, Imperial College of Science, Technology and Medicine Technical Report F/01/00164/REP, 2000.
36 M. Pehnt, *Int. J. Hydrogen Energy*, 2001, **26**, 91–101.
37 A. Primas, Life Cycle Inventories of new CHP systems, Swiss Centre for Life Cycle Inventories Technical Report ecoinvent report No. 20, 2007.
38 A. Burnham, Updated Vehicle Specifications in the GREET Vehicle-Cycle Model, Center for Transportation Research, Argonne National Laboratory technical report, 2012.

39 I. Staffell and A. Ingram, *Int. J. Hydrogen Energy*, 2010, **35**, 2491–2505.
40 P. Millet and S. Grigoriev, in *Renewable Hydrogen Technologies: Production, Purification, Storage, Applications and Safety*, ed. L. M. Gandia, G. Arzamendi and P. M. Dieguez, Elsevier B.V., 2013, ch. 2.
41 M. Müller, in *Fuel Cell Science and Engineering: Materials, Processes, Systems and Technology*, ed. D. Stolten and B. Emonts, Wiley-VCH Verlag & Co. KGaA, 2012, ch. 8.
42 Ecoinvent Centre, Ecoinvent data v2.0, 2007.
43 Rix Industries, Industrial Gas/Air Compressors 4VX: Compare Items, http://compressors.rixindustries.com/compare/commercial-compressors/industrial-gas-air-compressors-4vx?itemids=1038+1041.
44 A. J. Verhage, J. F. Coolegem, M. J. Mulder, M. H. Yildirim and F. A. de Bruijn, *Int. J. Hydrogen Energy*, 2013, **38**, 4714–4724.
45 R. Sookhoo, 2014, personal communication.
46 C. J. Barnhart and S. M. Benson, *Energy Environ. Sci.*, 2013, **6**, 1083.
47 C. J. Rydh and B. A. Sandén, *Energy Convers. Manage.*, 2005, **46**, 1957–1979.
48 U.S. DOE/Sandia National Laboratory, DOE Global Energy Storage Database, http://www.energystorageexchange.org/.
49 D. A. Notter, M. Gauch, R. Widmer, P. Wäger, A. Stamp, R. Zah and H.-J. Althaus, *Environ. Sci. Technol.*, 2010, **44**, 6550–6556.
50 G. Majeau-Bettez, T. R. Hawkins and A. H. Str, *Environ. Sci. Technol.*, 2011, **45**, 4548–4554.
51 M. K. Debe, *Nature*, 2012, **486**, 43–51.
52 A. Sarkar and R. Banerjee, *Int. J. Hydrogen Energy*, 2005, **30**, 867–877.
53 M. Neelis, H. van der Kooi and J. Geerlings, *Int. J. Hydrogen Energy*, 2004, **29**, 537–545.
54 F. Crotogino, S. Donadei, U. Bünger and H. Landinger, 18th World Hydrogen Energy Conference 2010 – WHEC 2010, 2010.
55 J.-P. Maton, L. Zhao and J. Brouwer, *Int. J. Hydrogen Energy*, 2013, **38**, 7867–7880.
56 T. Reddy and D. Linden, *Linden's Handbook of Batteries*, McGraw-Hill Prof Med/Tech, 4th edn, 2010, p. 1200.
57 M. Raugei, P. Fullana-i Palmer and V. Fthenakis, *Energy Policy*, 2012, **45**, 576–582.
58 D. Weissbach, G. Ruprecht, A. Huke, K. Czerski, S. Gottlieb and A. Hussein, *Energy*, 2013, **52**, 210–221.
59 B. Zakeri and S. Syri, *Renewable Sustainable Energy Rev.*, 2015, **42**, 569–596.
60 E. Barbour, I. A. G. Wilson, I. G. Bryden, P. G. McGregor, P. A. Mulheran and P. J. Hall, *Energy Environ. Sci.*, 2012, **5**, 5425.
61 N. Hughes and P. Agnolucci, *Comprehensive Renewable Energy*, Elsevier, 2012, pp. 65–95.
62 R. Loisel, A. Mercier, C. Gatzen, N. Elms and H. Petric, *Energy Policy*, 2010, **38**, 7323–7337.
63 R. Loisel, *International Journal of Electrical Power & Energy Systems*, 2012, **42**, 542–552.
64 N. Paine, F. R. Homans, M. Pollak, J. M. Bielicki and E. J. Wilson, *Energy Economics*, 2014, **46**, 10–19.
65 E. Barbour, I. G. Wilson, S. Gill and D. Infield, *IET Renew. Power Gen.*, 2013, **7**, 421–430.
66 C. Azcárate, R. Blanco, F. Mallor, R. Garde and M. Aguado, *Renewable Energy*, 2012, **47**, 103–111.

